

Power-Constrained Contrast Enhancement for Emissive Displays Based on Histogram Equalization

Chulwoo Lee, Chul Lee, *Student Member, IEEE*, Young-Yoon Lee, *Member, IEEE*, and Chang-Su Kim, *Senior Member, IEEE*

Abstract—A power-constrained contrast-enhancement algorithm for emissive displays based on histogram equalization (HE) is proposed in this paper. We first propose a log-based histogram modification scheme to reduce overstretching artifacts of the conventional HE technique. Then, we develop a power-consumption model for emissive displays and formulate an objective function that consists of the histogram-equalizing term and the power term. By minimizing the objective function based on the convex optimization theory, the proposed algorithm achieves contrast enhancement and power saving simultaneously. Moreover, we extend the proposed algorithm to enhance video sequences, as well as still images. Simulation results demonstrate that the proposed algorithm can reduce power consumption significantly while improving image contrast and perceptual quality.

Index Terms—Contrast enhancement, emissive displays, histogram equalization (HE), histogram modification (HM), image enhancement, low-power image processing.

I. INTRODUCTION

THE RAPID development of imaging technology has made it easier to take and process digital photographs. However, we often acquire low-quality photographs since lighting conditions and imaging systems are not ideal. Much effort has been made to enhance images by improving several factors, such as sharpness, noise level, color accuracy, and contrast. Among them, high contrast is an important quality factor for providing better experience of image perception to viewers. Various contrast-enhancement techniques have been developed. For example, histogram equalization (HE) is widely used to enhance low-contrast images [1].

Whereas a variety of contrast-enhancement techniques have been proposed to improve the qualities of general images, rel-

atively little effort has been made to adapt the enhancement process to the characteristics of display devices. Notice that, in addition to contrast enhancement, power saving is also an important issue in various multimedia devices, such as mobile phones and televisions. A large portion of power is consumed by display panels in these devices [2], [3], and this trend is expected to continue as display sizes are getting larger. Therefore, it is essential to develop an image processing algorithm, which is capable of saving power in display panels, as well as enhancing image contrast.

To design such a power-constrained contrast-enhancement (PCCE) algorithm, different characteristics of display panels should be taken into account. Modern display panels can be divided into emissive displays and nonemissive displays [4]. Cathode-ray tubes, plasma display panels (PDPs), organic light-emitting diode (OLED), and field emissive displays (FED) are emissive displays that do not require external light sources, whereas the thin-film transistor liquid crystal display (TFT-LCD) is a nonemissive one. Emissive displays have several advantages over nonemissive ones, including high contrast and low-power consumption. First, an emissive display can turn off individual pixels to express complete darkness and achieve a high contrast ratio. Second, in an emissive display, each pixel can be independently driven, and the power consumption of a pixel is proportional to its intensity level. Thus, an emissive display generally consumes less power than a nonemissive one, which should turn on a backlight regardless of pixel intensities. Due to these advantages, the OLED and the FED are considered as promising candidates for the next-generation display, although the TFT-LCD has been the first successful flat-panel display in the commercial market. In particular, the OLED is regarded as the most efficient emissive device in terms of power consumption [5]. Although the OLED is now used mainly for small panels in mobile devices, its mass-production technology is being rapidly developed, and larger OLED panels will be soon adopted in a wider range of devices, including televisions and computer monitors [6], [7].

Several image processing techniques for power saving in display panels have been recently proposed. These techniques focus on reducing backlight intensities for TFT-LCDs while preserving the same level of perceived quality. Choi *et al.* [8] increased pixel values to compensate for the brightness losses caused by a reduced backlight intensity. To compensate for the degraded contrast, Cheng *et al.* [2] truncated both ends of an image histogram and then stretched pixel intensities, and

Manuscript received October 15, 2010; revised February 19, 2011; accepted May 25, 2011. Date of publication June 13, 2011; date of current version December 16, 2011. This work was in part by the Mid-career Researcher Program through the National Research Foundation grant funded by the Ministry of Education, Science, and Technology under Grant 2010-0027541 and in part by Seoul Research and Business Development Program under Grant ST090818. Preliminary results of this paper were published in Proc. ICIP-2010, Sep. 2010. The associate editor coordinating the review of this manuscript and approving it for publication was Dr. Xin Li.

C. Lee, C. Lee, and C.-S. Kim are with the School of Electrical Engineering, Korea University, Seoul 136-713, Korea (e-mail: wiserain@korea.ac.kr; kayne@korea.ac.kr; changsukim@korea.ac.kr).

Y.-Y. Lee is with Samsung Electronics Company, Ltd., Suwon 442-742, Korea (e-mail: Euler.lee@samsung.com).

Color versions of one or more of the figures in this paper are available online at <http://ieeexplore.ieee.org>.

Digital Object Identifier 10.1109/TIP.2011.2159387

Iranli *et al.* [9] employed HE. Tsai *et al.* [3] decomposed an image into high- and low-frequency components and applied brightness compensation and contrast enhancement to these subband images. These techniques, however, have been devised for TFT-LCDs only and cannot be employed for emissive displays, in which the power consumption is affected by pixel values directly, rather than by a backlight intensity. To our knowledge, no attempt has been made to develop a contrast-enhancement algorithm tailored for emissive displays, in spite of their aforementioned advantages.

We propose a PCCE algorithm for emissive displays based on HE. First, we develop a histogram modification (HM) scheme, which reduces large histogram values to alleviate the contrast overstretching of the conventional HE technique. Then, we make a power-consumption model for emissive displays and formulate an objective function, consisting of the histogram-equalizing term and the power term. To minimize the objective function, we employ convex optimization techniques. Furthermore, we extend the proposed PCCE algorithm to enhance video sequences. Extensive simulation results show that the proposed algorithm provides high image contrast and good perceptual quality while reducing power consumption significantly.

The rest of this paper is organized as follows: Section II reviews conventional HE and HM techniques and proposes a log-based HM (LHM) scheme. Section III develops the power-consumption model for emissive displays and proposes the PCCE algorithm. Section IV describes how the PCCE algorithm can be extended to enhance video sequences. Section V presents experimental results. Finally, Section VI concludes this paper.

II. HE TECHNIQUES

Many contrast-enhancement techniques have been developed. HE is one of the most widely adopted approaches to enhance low-contrast images, which makes the histogram of light intensities of pixels within an image as uniform as possible [1]. It can increase the dynamic range of an image by deriving a transformation function adaptively. A variety of HE techniques have been proposed [10]–[17]. The main objective of this paper is to develop a power-constrained image enhancement framework, rather than to propose a sophisticated contrast-enhancement scheme. Thus, the proposed PCCE algorithm adopts the HE approach for its simplicity and effectiveness. Here, we first review conventional HE and HM techniques and then develop an LHM scheme, on which the proposed PCCE algorithm is based.

A. HE

In HE, we first obtain the histogram of pixel intensities in an input image. We represent the histogram with a column vector \mathbf{h} , whose k th element h_k denotes the number of pixels with intensity k . Then, the probability mass function p_k of intensity k is calculated by dividing h_k by the total number of pixels in the image. In other words

$$p_k = \frac{h_k}{1^t \mathbf{h}} \quad (1)$$

where $\mathbf{1}$ denotes the column vector, all elements of which are 1. The cumulative distribution function (CDF) c_k of intensity k is then given by

$$c_k = \sum_{i=0}^k p_i. \quad (2)$$

Let x_k denote the transformation function, which maps intensity k in the input image to intensity x_k in the output image. In HE, the transformation function is obtained by multiplying the CDF c_k by the maximum intensity of the output image [1], [17]. For a b -bit image, there are $2^b = L$ different intensity levels, and the transformation function is given by

$$x_k = \lfloor (L-1)c_k + 0.5 \rfloor \quad (3)$$

where $\lfloor a \rfloor$ is the floor operator, which returns the largest integer smaller than or equal to a . Thus, in (3), $(L-1)c_k$ is rounded off to the nearest integer since output intensities should be integers. Note that $b = 8$ and $L-1 = 255$, when an 8-bit image is considered.

If we ignore the rounding-off operation in (3), we can combine (2) and (3) into a recurrence equation, i.e.,

$$x_k - x_{k-1} = (L-1)p_k \quad \text{for } 1 \leq k \leq L-1 \quad (4)$$

with an initial condition $x_0 = (L-1)p_0$. This can be rewritten in vector notations as

$$\mathbf{D}\mathbf{x} = \bar{\mathbf{h}} \quad (5)$$

where $\mathbf{D} \in \mathbb{R}^{L \times L}$ is the differential matrix, i.e.,

$$\mathbf{D} = \begin{bmatrix} 1 & 0 & 0 & \cdots & 0 & 0 \\ -1 & 1 & 0 & \cdots & 0 & 0 \\ 0 & -1 & 1 & \cdots & 0 & 0 \\ \vdots & \vdots & \vdots & \ddots & \vdots & \vdots \\ 0 & 0 & 0 & \cdots & 1 & 0 \\ 0 & 0 & 0 & \cdots & -1 & 1 \end{bmatrix} \quad (6)$$

and $\bar{\mathbf{h}}$ is the normalized column vector of \mathbf{h} , given by

$$\bar{\mathbf{h}} = \frac{L-1}{1^t \mathbf{h}} \mathbf{h}. \quad (7)$$

B. HM

The conventional HE algorithm has several drawbacks. First, when a histogram bin has a very large value, the transformation function gets an extreme slope. In other words, note from (4) that the transformation function has sharp transition between x_{k-1} and x_k when h_k or, equivalently, p_k is large. This can cause contrast overstretching, mood alteration, or contour artifacts in the output image. Second, particularly for dark images, HE transforms very low intensities to brighter intensities, which may boost noise components as well, degrading the resulting image quality. Third, the level of contrast enhancement cannot be controlled since the conventional HE is a fully automatic algorithm without any parameter.

To overcome these drawbacks, many techniques have been proposed. One of those is HM. In general, HM is the technique

that employs the histogram information in an input image to obtain the transformation function [18], [19]. Thus, HE can be regarded as a special case of HM. A recent approach to HM [16], [17] modifies the input histogram before the HE procedure to reduce extreme slopes in the transformation function, instead of the direct control of the output histogram. For instance, Wang and Ward [16] clamped large histogram values and then modified the resulting histogram further using the power law. Also, Arici *et al.* [17] reduced the histogram values for large smooth areas, which often correspond to background regions, and mixed the resulting histogram with the uniform histogram.

In this recent approach to HM, the first step can be expressed by a vector-converting operation $\mathbf{m} = f(\mathbf{h})$, where $\mathbf{m} = [m_0, m_1, \dots, m_{L-1}]^t$ denotes the modified histogram. Then, the desired transformation function $\mathbf{x} = [x_0, x_1, \dots, x_{L-1}]^t$ can be obtained by solving

$$\mathbf{D}\mathbf{x} = \bar{\mathbf{m}} \quad (8)$$

which is the same HE procedure as in (5), except that $\bar{\mathbf{m}}$ is used instead of $\bar{\mathbf{h}}$, where $\bar{\mathbf{m}}$ is the normalized column vector of \mathbf{m} , i.e.,

$$\bar{\mathbf{m}} = \frac{L-1}{1^t \mathbf{m}} \mathbf{m}. \quad (9)$$

C. LHM

We develop an HM scheme using a logarithm function, which is monotonically increasing and can reduce large values effectively. In [20], Drago *et al.* demonstrated that a logarithm function can successfully reduce the dynamic ranges of high-dynamic-range images while preserving the details. We exploit this property and apply a logarithm function to our HM scheme, which is called LHM.

We use the following logarithm function to convert the input histogram value h_k to a modified histogram value m_k :

$$m_k = \frac{\log(h_k \cdot h_{\max} \cdot 10^{-\mu} + 1)}{\log(h_{\max}^2 \cdot 10^{-\mu} + 1)} \quad (10)$$

where h_{\max} denotes the maximum element within the input histogram \mathbf{h} and μ is the parameter that controls the level of HM. As μ gets larger, $h_k \cdot h_{\max} \cdot 10^{-\mu}$ in (10) becomes a smaller number. Therefore, a large μ makes m_k almost linearly proportional to h_k since $\log(1+x) \simeq x$ for a small x . Thus, the histogram is less strongly modified. On the other hand, as μ gets smaller, $h_{\max} \cdot 10^{-\mu}$ becomes dominant and

$$\begin{aligned} \log(h_k \cdot h_{\max} \cdot 10^{-\mu} + 1) &\simeq \log(h_k) + \log(h_{\max} \cdot 10^{-\mu}) \\ &\simeq \log(h_{\max} \cdot 10^{-\mu}). \end{aligned} \quad (11)$$

Consequently, m_k becomes a constant regardless of h_k , making the modified histogram uniform. In this way, a smaller μ results in stronger HM.

Fig. 1(a) illustrates how the proposed LHM scheme modifies an input histogram according to parameter μ , and Fig. 1(b) plots the corresponding transformation functions, which are obtained by solving (8). In this test, the ‘‘Door’’ image in Fig. 1(c) is used as the input image. We see that LHM reduces the large peak of the input histogram around the pixel value of 70 and thus relaxes

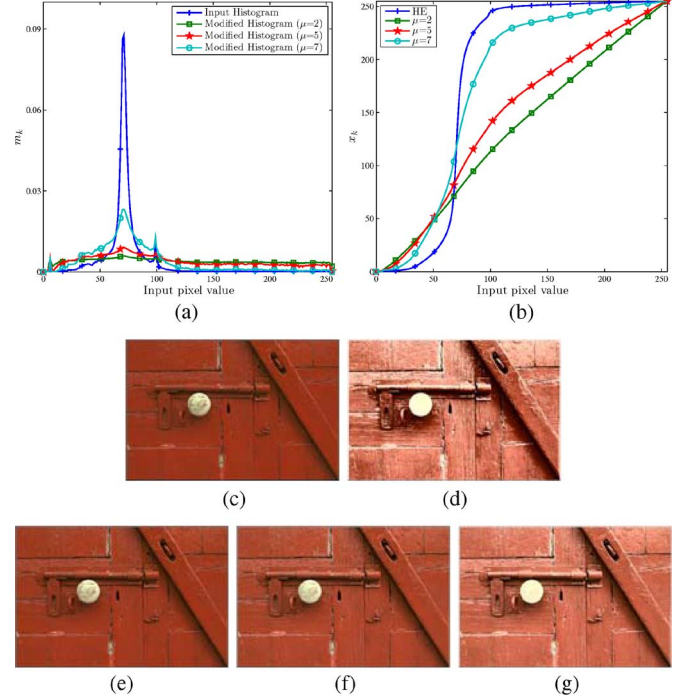


Fig. 1. Illustration of LHM: (a) The input and modified histograms of the test image in (c), in which each histogram is normalized so that the sum of all elements is 1. (b) The corresponding transformation functions. [(d)–(g)] The output images. (a) Histograms. (b) Transformation functions. (c) Input image. (d) HE. (e) $\mu = 2$. (f) $\mu = 5$. (g) $\mu = 7$.

the steep slope in the transformation function of the conventional HE algorithm. Fig. 1(d)–(g) compare the output images of the conventional HE algorithm and the proposed LHM scheme. Because of the steep slope, the conventional HE overstretchs the contrast of the background, but it maps the input-pixel range [100, 255] to the narrow output range of variation about 10 only, wiping out the details on the door knob. On the other hand, the proposed algorithm with $\mu = 5$ yields less artifacts on the door knob while enhancing the details on the background region. It is also observed from Fig. 1(a) that LHM modifies the histogram more strongly as μ gets smaller. In the extreme case when $\mu = -\infty$, the modified histogram becomes uniformly distributed. In the other extreme case when $\mu = \infty$, the histogram is not modified at all. Therefore, by controlling the single parameter μ , LHM can obtain the transformation function, which varies between the identity function and the conventional HE result.

III. PCCE

Here, we propose the PCCE algorithm. Fig. 2 shows an overview of the proposed algorithm. We first gather the histogram information \mathbf{h} from an input image and apply the LHM scheme to \mathbf{h} to obtain the modified histogram \mathbf{m} . Without power constraint, we can solve equation $\mathbf{D}\mathbf{x} = \bar{\mathbf{m}}$ in (8) to get the transformation function \mathbf{x} . However, we design an objective function, which consists of power-constraint and contrast-enhancement terms. We then express the objective function in terms of variable $\mathbf{y} = \mathbf{D}\mathbf{x}$. Based on the convex optimization theory [21], we find the optimal \mathbf{y} that minimizes the objective function. Finally, we construct the transformation function \mathbf{x}

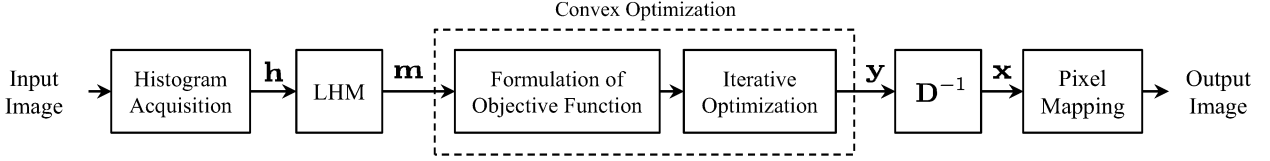


Fig. 2. Flow diagram of the proposed PCCE algorithm.

from \mathbf{y} via $\mathbf{x} = \mathbf{D}^{-1}\mathbf{y}$ and use \mathbf{x} to transform the input image to the output image.

A. Power Model for Emissive Displays

We model the power consumption in an emissive display panel that is required to display an image. In [22], Dong *et al.* presented a pixel-level power model for an OLED module. According to their experimental results, power P to display a single-color pixel can be modeled by

$$P = w_0 + w_r R^\gamma + w_g G^\gamma + w_b B^\gamma \quad (12)$$

where R , G , and B are the red, green, and blue values of the pixel. Exponent γ is due to the gamma correction of the color values in the sRGB format. A typical γ is 2.2 [23]. In other words, after transforming the color values into luminous intensities in the linear RGB format, we obtain a linear relation between the power and the luminous intensities. Also, w_0 accounts for static power consumption, which is independent of pixel values, and w_r , w_g , and w_b are weighting coefficients that express the different characteristics of red, green, and blue subpixels.

In this paper, we alter pixel values to save power in a display panel. Therefore, we ignore parameter w_0 for static power consumption. Then, we model the total dissipated power (TDP) for displaying a color image by

$$\text{TDP} = \sum_{i=0}^{N-1} (w_r R_i^\gamma + w_g G_i^\gamma + w_b B_i^\gamma) \quad (13)$$

where N denotes the number of pixels in the image and (R_i, G_i, B_i) denotes the RGB color vector of the i th pixel. The weighting coefficients w_r , w_g , and w_b are inversely proportional to the subpixel efficiencies, which depend on the physical characteristics of a specific display panel. A blue subpixel generally consumes more power than red and green subpixels to display the same output level due to its low efficiency. For example, in a particular OLED panel in a mobile phone, the weighting ratios are about $w_r : w_g : w_b = 70 : 115 : 154$. However, we note that different display panels have different weighting coefficients.

For a grayscale image, the TDP is similarly modeled by

$$\text{TDP} = \sum_{i=0}^{N-1} Y_i^\gamma \quad (14)$$

where Y_i is the gray level of the i th pixel. Let us recall the notations in the last section; there are h_k pixels with gray level k in the input image, and these pixels are assigned gray level x_k in the output image by the transformation function. Therefore, the TDP in (14) can be compactly written in vector notations as

$$\text{TDP} = \sum_{k=0}^{L-1} h_k x_k^\gamma = \mathbf{h}^t \phi^\gamma(\mathbf{x}) \quad (15)$$

where $\phi^\gamma(\mathbf{x}) = [x_0^\gamma, x_1^\gamma, \dots, x_{L-1}^\gamma]^t$ and \mathbf{h} is the histogram vector whose k th element is h_k .

Notice that the power model in (13) or (14) is applicable to not only the OLED but also other emissive displays. In [24], Rose *et al.* analyzed the power-consumption characteristics of several displays. First, in PDPs, the sustain power dominates the whole power consumption. The sustain power is proportional to the average picture level ω_{APL} , which is the average of luminous intensities of all pixels in an image. The average picture level ω_{APL} is, in turn, linearly proportional to the TDP in (14) since it is obtained by dividing the TDP by the number of pixels N . Therefore, the TDP in (14) can model the power consumption in the PDP as well. Similarly, it can model the power consumption in the FED, in which the power consumption is also proportional to ω_{APL} .

B. Constrained Optimization Problem

We save the power in an emissive display by incorporating the power model in (15) into the HE procedure. We have two contradictory goals, i.e., we attempt to enhance the image contrast by equalizing the histogram, but we also try to decrease the power consumption by reducing the histogram values for large intensities. These goals can be stated as a constrained optimization problem, i.e.,

$$\begin{aligned} & \text{minimize} \quad \|\mathbf{D}\mathbf{x} - \bar{\mathbf{m}}\|^2 + \alpha \mathbf{h}^t \phi^\gamma(\mathbf{x}) \\ & \text{subject to} \quad x_0 = 0, \\ & \quad \quad \quad x_{L-1} = L - 1, \\ & \quad \quad \quad \mathbf{D}\mathbf{x} \succeq \mathbf{0}. \end{aligned} \quad (16)$$

The objective function $\|\mathbf{D}\mathbf{x} - \bar{\mathbf{m}}\|^2 + \alpha \mathbf{h}^t \phi^\gamma(\mathbf{x})$ has two terms, i.e., $\|\mathbf{D}\mathbf{x} - \bar{\mathbf{m}}\|^2$ is the histogram-equalizing term in (8) and $\mathbf{h}^t \phi^\gamma(\mathbf{x})$ is the power term in (15). By minimizing the sum of these two terms, we attempt to improve the image contrast and reduce the power consumption simultaneously. Here, α is a user-controllable parameter, which determines the balance between the two terms.

There are three constraints in our optimization problem in (16). The two equality constraints $x_0 = 0$ and $x_{L-1} = L - 1$ state that the minimum and maximum intensities should be maintained without changes. In other words, if a display can express L different intensity levels, the output range of the transformation function should also be $[0, L - 1]$ to exploit the full dynamic range. The inequality constraint $\mathbf{D}\mathbf{x} \succeq \mathbf{0}$ indicates that the transformation function \mathbf{x} should be monotonic, i.e.,

$x_k \geq x_{k-1}$ for every k . Note that $\mathbf{a} \succeq \mathbf{0}$ denotes that all elements in vector \mathbf{a} are greater than or equal to 0. Without this monotonic constraint, the solution to the optimization problem may yield a transformation function, which reverses the intensity ordering of pixels and yields visually annoying artifacts in the output image.

C. Solution to the Optimization Problem

As mentioned in Section III-A, exponent γ in the power term $\mathbf{h}^t \phi^\gamma(\mathbf{x})$ is due to the gamma correction, and a typical γ is 2.2. For generality, let us assume that γ is any number greater than or equal to 1. Then, the power term $\mathbf{h}^t \phi^\gamma(\mathbf{x})$ is a convex function of \mathbf{x} , and the problem in (16) becomes a convex optimization problem [21]. Based on the convex optimization theory, we develop the PCCE algorithm to yield the optimal solution to the problem.

According to the minimum-value constraint in (16), x_0 is fixed to 0 and is not treated as a variable. Thus, the transformation function can be rewritten as $\mathbf{x} = [x_1, x_2, \dots, x_{L-1}]^t$ after removing x_0 from the original \mathbf{x} . Similarly, the dimensions of $\bar{\mathbf{m}}$, \mathbf{h} , and $\phi^\gamma(\mathbf{x})$ are reduced to $L-1$ by removing the first elements, respectively, and \mathbf{D} has a reduced size $(L-1) \times (L-1)$ by removing the first row and the first column.

Then, we reformulate the optimization problem by the change of variable $\mathbf{y} = \mathbf{D}\mathbf{x}$. Each element y_k in the new variable \mathbf{y} is the difference between two output-pixel intensities, i.e., $y_k = x_k - x_{k-1}$. Thus, \mathbf{y} is called the differential vector. Then, $\mathbf{x} = \mathbf{D}^{-1}\mathbf{y}$, where

$$\mathbf{D}^{-1} = \begin{bmatrix} 1 & 0 & \cdots & 0 & 0 \\ 1 & 1 & \cdots & 0 & 0 \\ \vdots & \vdots & \ddots & \vdots & \vdots \\ 1 & 1 & \cdots & 1 & 0 \\ 1 & 1 & \cdots & 1 & 1 \end{bmatrix} \in \mathbb{R}^{(L-1) \times (L-1)}. \quad (17)$$

By substituting variable $\mathbf{x} = \mathbf{D}^{-1}\mathbf{y}$ and expressing the maximum-value constraint in terms of \mathbf{y} , (16) can be reformulated as

$$\begin{aligned} & \text{minimize} \quad \|\mathbf{y} - \bar{\mathbf{m}}\|^2 + \alpha \mathbf{h}^t \phi^\gamma(\mathbf{D}^{-1}\mathbf{y}) \\ & \text{subject to} \quad \mathbf{1}^t \mathbf{y} = L-1, \\ & \quad \mathbf{y} \succeq \mathbf{0}. \end{aligned} \quad (18)$$

To solve the optimization problem, we define the Lagrangian cost function, i.e.,

$$J(\mathbf{y}, \nu, \boldsymbol{\lambda}) = \|\mathbf{y} - \bar{\mathbf{m}}\|^2 + \alpha \mathbf{h}^t \phi^\gamma(\mathbf{D}^{-1}\mathbf{y}) + \nu (\mathbf{1}^t \mathbf{y} - (L-1)) - \boldsymbol{\lambda}^t \mathbf{y} \quad (19)$$

where $\nu \in \mathbb{R}$ and $\boldsymbol{\lambda} = [\lambda_1, \lambda_2, \dots, \lambda_{L-1}] \in \mathbb{R}^{L-1}$ are Lagrangian multipliers for the constraints. Then, the optimal \mathbf{y} can be obtained by solving the Karush–Kuhn–Tucker conditions [21], i.e.,

$$\mathbf{1}^t \mathbf{y} = L-1 \quad (20)$$

$$\mathbf{y} \succeq \mathbf{0} \quad (21)$$

$$\boldsymbol{\lambda} \succeq \mathbf{0} \quad (22)$$

$$\boldsymbol{\Lambda} \mathbf{y} = \mathbf{0} \quad (23)$$

$$2(\mathbf{y} - \bar{\mathbf{m}}) + \alpha \gamma \mathbf{D}^{-t} \mathbf{H} \phi^{\gamma-1}(\mathbf{D}^{-1}\mathbf{y}) + \nu \mathbf{1} - \boldsymbol{\lambda} = \mathbf{0} \quad (24)$$

where $\boldsymbol{\Lambda} = \text{diag}(\boldsymbol{\lambda})$ and $\mathbf{H} = \text{diag}(\mathbf{h})$.

We first expand the vector notations in (24) to obtain a system of equations and subtract the i th equation from the $(i+1)$ th one to eliminate ν . Then, we have a recursive system, i.e.,

$$y_{i+1} = y_i + \bar{m}_{i+1} - \bar{m}_i + \frac{\alpha \gamma}{2} h_i \left(\sum_{k=1}^i y_k \right)^{\gamma-1} + \frac{\lambda_{i+1} - \lambda_i}{2} \quad \text{for } 1 \leq i \leq L-2. \quad (25)$$

In the Appendix, we show that all λ_i values can be eliminated from the recursion in (25) using (21)–(23) and that all y_i values can be expressed in terms of a single variable z . More specifically, each y_i is a monotonically increasing function of z , given by $y_i = g_i(z)$. Then, the remaining step is to determine z that satisfies the maximum-value constraint in (20). To this end, we form a function, i.e.,

$$f(z) = \mathbf{1}^t \mathbf{y} - (L-1) = \sum_{i=1}^{L-1} g_i(z) - (L-1) \quad (26)$$

and find a solution to $f(z) = 0$. Since $f(z)$ is monotonically increasing, there exists a unique solution to $f(z) = 0$. In this paper, we employ the secant method [25] to find the unique solution iteratively. Let $z^{(n)}$ denote the value of z at the n th iteration. By applying the secant formula, i.e.,

$$z^{(n)} = z^{(n-1)} - \frac{z^{(n-1)} - z^{(n-2)}}{f(z^{(n-1)}) - f(z^{(n-2)})} f(z^{(n-1)}), \quad n = 2, 3, \dots \quad (27)$$

iteratively until the convergence, we obtain solution z . From z , we can compute all elements in \mathbf{y} since $y_i = g_i(z)$. Finally, the transformation function $\mathbf{x} = \mathbf{D}^{-1}\mathbf{y}$ is the optimal solution to the original problem in (16), which enhances the contrast and saves the power consumption simultaneously subject to the minimum-value, maximum-value, and monotonic constraints.

Parameter α in the objective function in (18) determines the relative contributions of the histogram-equalizing term $\|\mathbf{y} - \bar{\mathbf{m}}\|^2$ and the power term $\mathbf{h}^t \phi^\gamma(\mathbf{D}^{-1}\mathbf{y})$. These two terms, however, have different orders of magnitude in general. Whereas \mathbf{y} and $\bar{\mathbf{m}}$ are not affected by the resolution of an input image, histogram values in \mathbf{h} depend on the image resolution. Moreover, the power term is generally proportional to the average luminance value of the input image. It is convenient to compensate the unbalance between the two terms by dividing the power term by the image resolution and the average luminance value. More specifically, we change the variable by

$$\beta = \alpha \times \sum_{i=0}^{N-1} Y_{\text{input},i} \quad (28)$$

where $Y_{\text{input},i}$ is the gray level of the i th pixel in the input image. Then, we control β instead of α .

For example, Fig. 3 shows the results of the proposed PCCE algorithm at various β values. In this test, the “Door” image in Fig. 1(c) is also used as the input image, the LHM parameter μ is set to 5, and γ is set to 2.2. In Fig. 3(a), when $\beta = 0$, the power

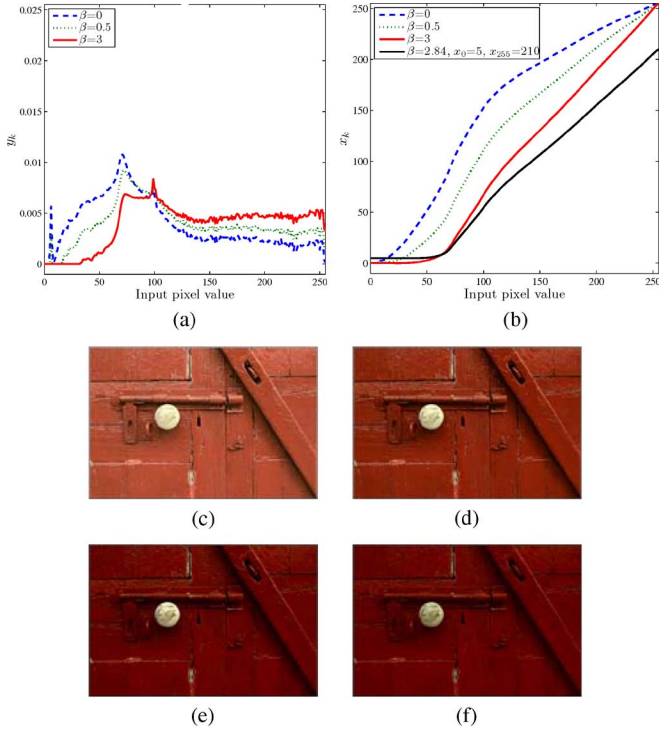


Fig. 3. PCCE results on the “Door” image at various β values. In the black curve in (b) and the corresponding output image in (f), generalized minimum- and maximum-value constraints $x_0 = 5$ and $x_{255} = 210$ are used. In the other cases, the original constraints $x_0 = 0$ and $x_{255} = 255$ are used. Note that (c) is the result without the power constraint, and thus, it is exactly the same as Fig. 1(f). (a) Differential vectors \mathbf{y} . (b) Transformation functions \mathbf{x} . (c) $\beta = 0$. (d) $\beta = 0.5$. (e) $\beta = 3$. (f) $\beta = 2.84$, $x_0 = 5$, and $x_{255} = 210$.

term is not considered in (18), and we obtain the differential vector $\mathbf{y} = \bar{\mathbf{m}}$. As β gets larger, the elements y_k for low pixel values k decrease, whereas y_k values for high k values increase. As shown in Fig. 3(b), these changes in \mathbf{y} lower the transformation function, reducing the power consumption. A bigger β saves more power. Without the power constraint ($\beta = 0$), the TDP is 9.28×10^9 . At $\beta = 0.5$ and 3 , the proposed algorithm reduces the TDP to 3.55×10^9 and 1.11×10^9 , respectively. In this way, the proposed algorithm determines the transformation function that balances the requirements of power saving and contrast enhancement optimally. Furthermore, the amount of power saving can be controlled by the single parameter β .

Note that the output black and white levels may not be the same as the input black and white levels in some applications. The proposed PCCE algorithm can be straightforwardly modified to handle such cases. Specifically, instead of the minimum- and maximum-value constraints in (16), we can use generalized constraints $x_0 = l_{\min}$ and $x_{L-1} = l_{\max}$ to derive the transformation function, which maps the input dynamic range $[0, L-1]$ to the output dynamic range $[l_{\min}, l_{\max}]$. For instance, Fig. 3(b) also shows the transformation function with constraints $x_0 = 5$ and $x_{255} = 210$. Parameter β is set to 2.84 to consume the same TDP as the red curve ($x_0 = 0, x_{255} = 255, \beta = 3$) in Fig. 3(b). Comparing the output images in Fig. 3(e) and (f), we see that the new constraints reduce the dynamic range and degrade the

overall contrast. In the remainder of this paper, the original constraints are employed to exploit the full dynamic range.

D. Special Case of $\gamma = 2$

In [26], although a typical value of γ is 2.2 , we approximated γ to 2 to make TDP in (15) a quadratic function, which is easier to analyze than the general convex function. More specifically, when $\gamma = 2$, the objective function in (16) becomes a quadratic function, given by

$$J_q(\mathbf{x}) = (\mathbf{D}\mathbf{x} - \bar{\mathbf{m}})^t(\mathbf{D}\mathbf{x} - \bar{\mathbf{m}}) + \alpha \mathbf{x}^t \mathbf{H} \mathbf{x} \quad (29)$$

$$= \mathbf{x}^t \mathbf{D}^t \mathbf{D} \mathbf{x} - 2\mathbf{x}^t \mathbf{D}^t \bar{\mathbf{m}} + \bar{\mathbf{m}}^t \bar{\mathbf{m}} + \alpha \mathbf{x}^t \mathbf{H} \mathbf{x}. \quad (30)$$

By differentiating $J_q(\mathbf{x})$ with respect to \mathbf{x} and setting it to $\mathbf{0}$, we obtain the following transformation function:

$$\mathbf{x} = (\mathbf{D}^t \mathbf{D} + \alpha \mathbf{H})^{-1} \mathbf{D}^t \bar{\mathbf{m}}. \quad (31)$$

Therefore, in the special case of $\gamma = 2$, the transformation function is given in a closed form, without requiring the convex optimization procedure.

However, the solution in (31) does not satisfy the constraints in (16) in general, particularly the maximum-value and monotonic constraints. In [26], we developed a scheme that augments matrix \mathbf{D} and vector $\bar{\mathbf{m}}$ to enforce the maximum-value constraint. However, [26] still may yield a transformation function, which reverses the ordering of pixel intensities in the output image. The reverse mapping can degrade the image quality severely. On the contrary, the proposed PCCE algorithm always provides the optimal transformation function, which satisfies all the constraints. Moreover, the proposed algorithm can be employed for any $\gamma \geq 1$.

IV. PCCE FOR VIDEO SEQUENCES

We extend the proposed PCCE algorithm to enhance video sequences. The proposed algorithm provides a power-reduced output image using the power-control parameter β . We can apply the proposed algorithm with fixed β to each frame in a video sequence. However, a typical video sequence is composed of frames with fluctuating brightness levels. Experiments in Section V-B will show that a bright frame can be enhanced with large β to save power aggressively, whereas a dark frame can be severely degraded if its overall brightness is reduced further with the same β . Therefore, we develop a scheme that determines β adaptively according to the brightness level of each frame.

For each frame, we first set the target power consumption TDP_{out} based on the input power consumption $\text{TDP}_{\text{in}} = \sum_{k=0}^{L-1} h_k \cdot k^\gamma$ and then control parameter β to achieve TDP_{out} . Specifically, we set

$$\text{TDP}_{\text{out}} = \kappa \cdot \text{TDP}_{\text{in}} \quad (32)$$

where κ is the power-reduction ratio. When $\kappa = 1$, the proposed algorithm saves no power during the contrast enhancement. On the other hand, when κ is smaller, the proposed algorithm darkens the output frame and decreases the power consumption.

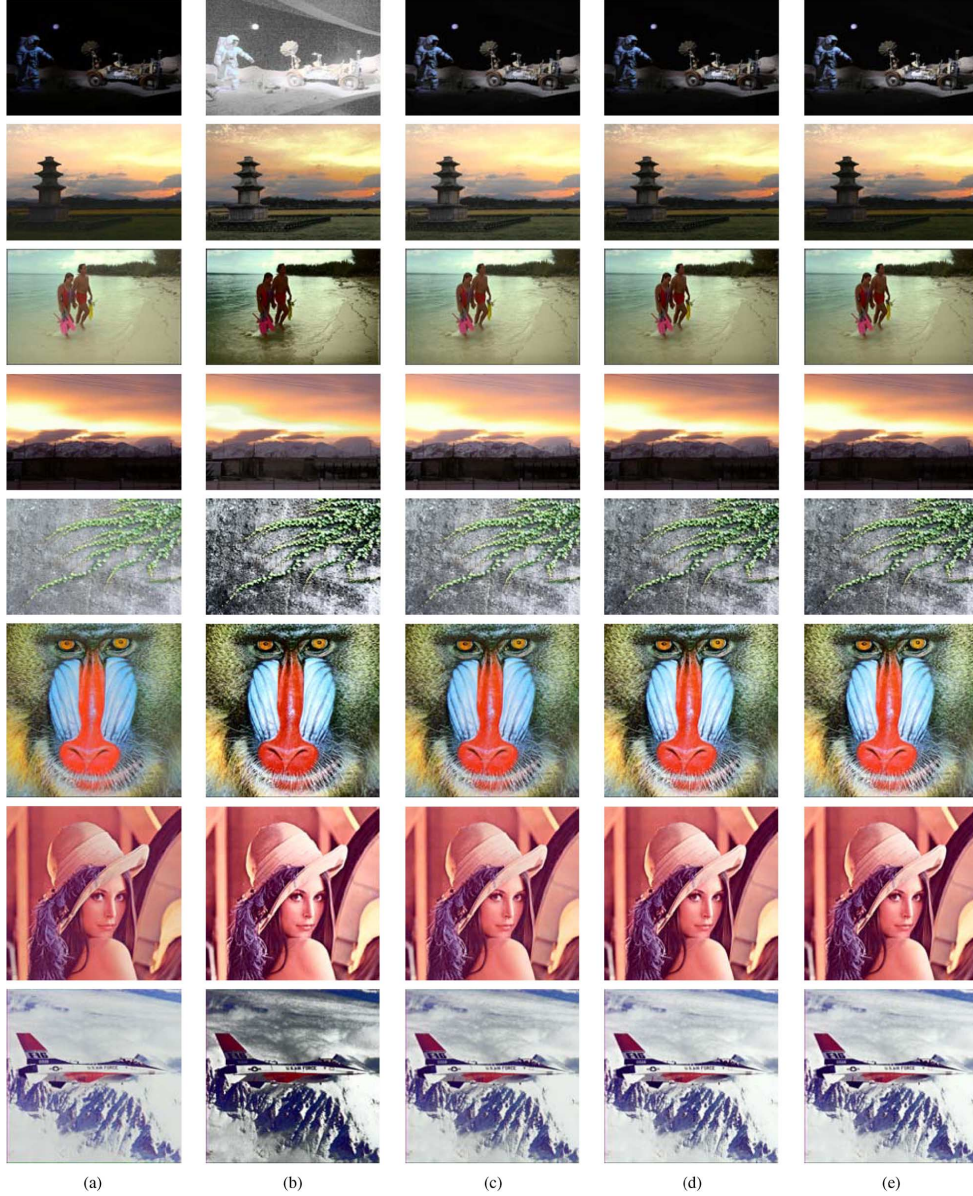


Fig. 4. Contrast enhancement results on the test images “Moon,” “Pagoda,” “Beach,” “Sunset,” “Ivy,” “Baboon,” “Lena,” and “F-16”: (a) Original input images, (b) the conventional HE algorithm, (c) WAHE [17], (d) PCCE with adapted μ , and (e) PCCE with $\mu = 5$. The proposed PCCE algorithm is tested without the power constraint ($\beta = 0$).

The power model in Section III-A indicates that a bright frame consumes more power than a dark frame. Therefore, more power saving can be achieved for a brighter frame, and the power-reduction ratio κ in (32) can be set to a smaller value. On the other hand, the ratio for a dark frame should be close to 1 since even a small power reduction may yield poor image quality by reducing the contrast further and erasing details. Based on these observations, we set the power-reduction ratio κ by

$$\kappa = \left(1 - \frac{\bar{Y}}{L-1}\right)^\rho \quad (33)$$

where \bar{Y} denotes the average gray level of an input frame and ρ is a user-controllable parameter. For a bright input frame with high \bar{Y} , κ is set to a small value to achieve aggressive power

saving. On the contrary, for a dark input frame with low \bar{Y} , κ is set to be close to 1 to avoid the brightness reduction.

To summarize, given an input frame, we determine the target power consumption TDP_{out} using (32) and (33). Then, we find parameter β to achieve TDP_{out} . Since TDP_{out} is inversely proportional to β , we can easily obtain the desired β using the bisection method [27], which iteratively halves a candidate range of the solution into two subdivisions and selects the subdivision containing the solution. Thus, in the video enhancement, β is automatically determined, and the only power-control parameter is ρ in (33). Note that, for the same \bar{Y} , larger ρ yields smaller κ and saves more power.

V. EXPERIMENTAL RESULTS

We evaluate the performance of the proposed algorithm on ten test images, i.e., “Door,” “Moon,” “Pagoda,” “Beach,” “

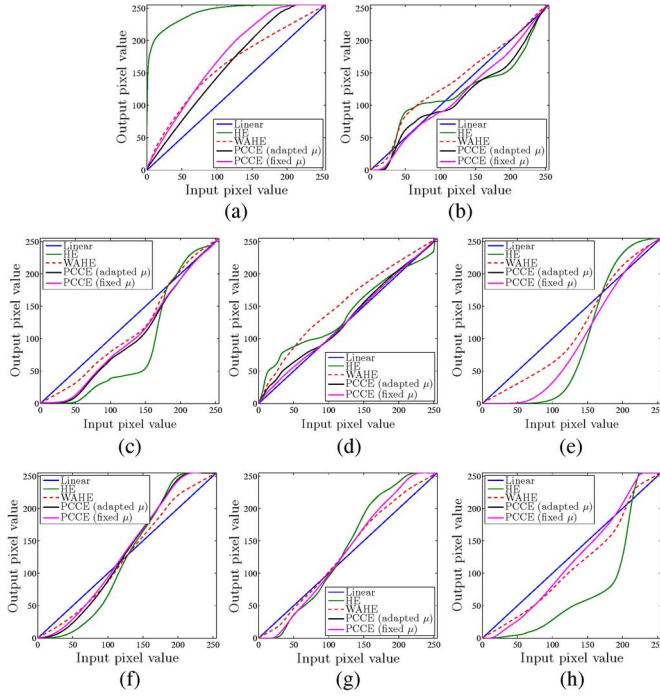


Fig. 5. Transformation functions used to obtain the output images in Fig. 4. (a) Moon. (b) Pagoda. (c) Beach. (d) Sunset. (e) Ivy. (f) Baboon. (g) Lena. (h) F-16.

“Sunset,” “Ivy,” “Baboon,” “Lena,” “F-16,” and “Eiffel Tower.” These test images are shown in Figs. 1, 4, and 10. “Beach” and “Door” are from Kodak Lossless True Color Image Suite,¹ “Baboon,” “Lena,” and “F-16” are from the USC-SIPI database,² and the others are taken with a commercial digital camera and resized. The resolution of “Eiffel Tower” is 480×720 , those of the USC-SIPI images are 512×512 , and those of the others are 720×480 . We process only the luminance components in the experiments. More specifically, given a color image, we convert it to the YUV color space and then process only the Y-component without modifying the U- and V-components. Therefore, the TDP is also measured for the Y-component only using (14). In all experiments, γ is set to 2.2.

A. Contrast Enhancement Without Power Constraint

First, we compare the proposed PCCE algorithm without the power constraint ($\beta = 0$) with the conventional HE and HM techniques. Fig. 4 shows the processed images obtained by the conventional HE algorithm, the weighted approximated HE (WAHE) algorithm [17], and the proposed PCCE algorithm ($\beta = 0$). The proposed algorithm is tested in two ways. In Fig. 4(d), the user-controllable parameter μ for LHM in (10) is set to 2, 6.5, 5.5, 6.5, 5, 5.5, 5, and 5 for the eight test images, respectively, to achieve the best subjective qualities. On the other hand, in Fig. 4(e), μ is fixed to 5. For the WAHE results in Fig. 4(c), parameter g is adapted for each image to achieve the best subjective quality. Fig. 5 shows the transformation functions, which are used to obtain the images in Fig. 4.

We observe from Fig. 4(b) that the conventional HE algorithm causes excessive contrast stretching. In the “Moon” image, hidden noises become visible, degrading the image quality severely. This noise amplification is due to the steep slope of the transformation function near intensity 0, as shown in Fig. 5. The contrast overstretching suppresses the overall brightness of the “Beach” image. The transformation function reduces the input-pixel range $[0, 150]$ to the output-pixel range $[0, 50]$ by extending the contrast around the input-pixel intensity 170, which corresponds to the background area. Also, contour artifacts are observed in “Sunset.” In general, the conventional HE algorithm often produces unsatisfactory results, including amplified noises, contour artifacts, detail losses, and mood alteration.

Compared with the conventional HE, both WAHE and the proposed algorithm reduce artifacts by alleviating abrupt changes in the transformation functions, as shown in Fig. 4(c) and (d). WAHE exploits spatial variance information to reduce large histogram values, based on the observation that peaks in histograms usually come from background regions. Specifically, WAHE skips repeated pixel intensities during the construction of an input histogram to focus on the contrast enhancement of textured regions. Thus, it can enhance object details, whereas it may degrade background details. For example, on the “Pagoda” image, WAHE improves the contrast of the tower but loses the details in the clouds. Similarly, since the wall in the “Ivy” image has small intensity variations, its contrast is not enhanced by WAHE significantly.

The proposed PCCE algorithm provides comparable or better results than WAHE on all test images, as shown in Fig. 4(d). On the “Moon,” “Beach,” “Sunset,” “Baboon,” “Lena,” and “F-16” images, the proposed algorithm and WAHE produce similar results. However, on the “Pagoda” and “Ivy” images, the proposed algorithm yields better perceptual quality than WAHE. Notice that the proposed algorithm enhances the clouds in “Pagoda” and the patterns on the wall in “Ivy” more clearly. In Fig. 4(e), we fix the LHM parameter μ to 5. Except for slight differences in the “Pagoda” image, the output images with the fixed μ are almost indiscernible from those with the adapted μ values in Fig. 4(d). Experiments on various other images also confirm that $\mu = 5$ is a reliable choice. Therefore, in the following experiments, μ is set to 5 unless otherwise specified.

B. Contrast Enhancement With Power Constraint

Next, we evaluate the performance of the proposed PCCE algorithm with the power constraint ($\beta > 0$). Fig. 6 shows the output images obtained by the proposed algorithm at different β values. The images in Fig. 6(a) are exactly the same as those in Fig. 4(e). As β gets larger, the overall brightness of the output images decreases, but the image contrast is relatively well preserved. Note that the perceptual quality and the subjective contrast of the output images at $\beta = 0.5$ are almost the same as those at $\beta = 0$. In particular, when these images are displayed on OLED panels, it is hard to distinguish the case without the power constraint ($\beta = 0$) from the case with the power constraint ($\beta > 0$) unless β is set to be very high. Fig. 6(e) shows the output images when β has a very high value of 15. Even in this case, the originally bright images “Ivy” and “F-16” retain

¹<http://r0k.us/graphics/kodak/>

²<http://sipi.usc.edu/database/>

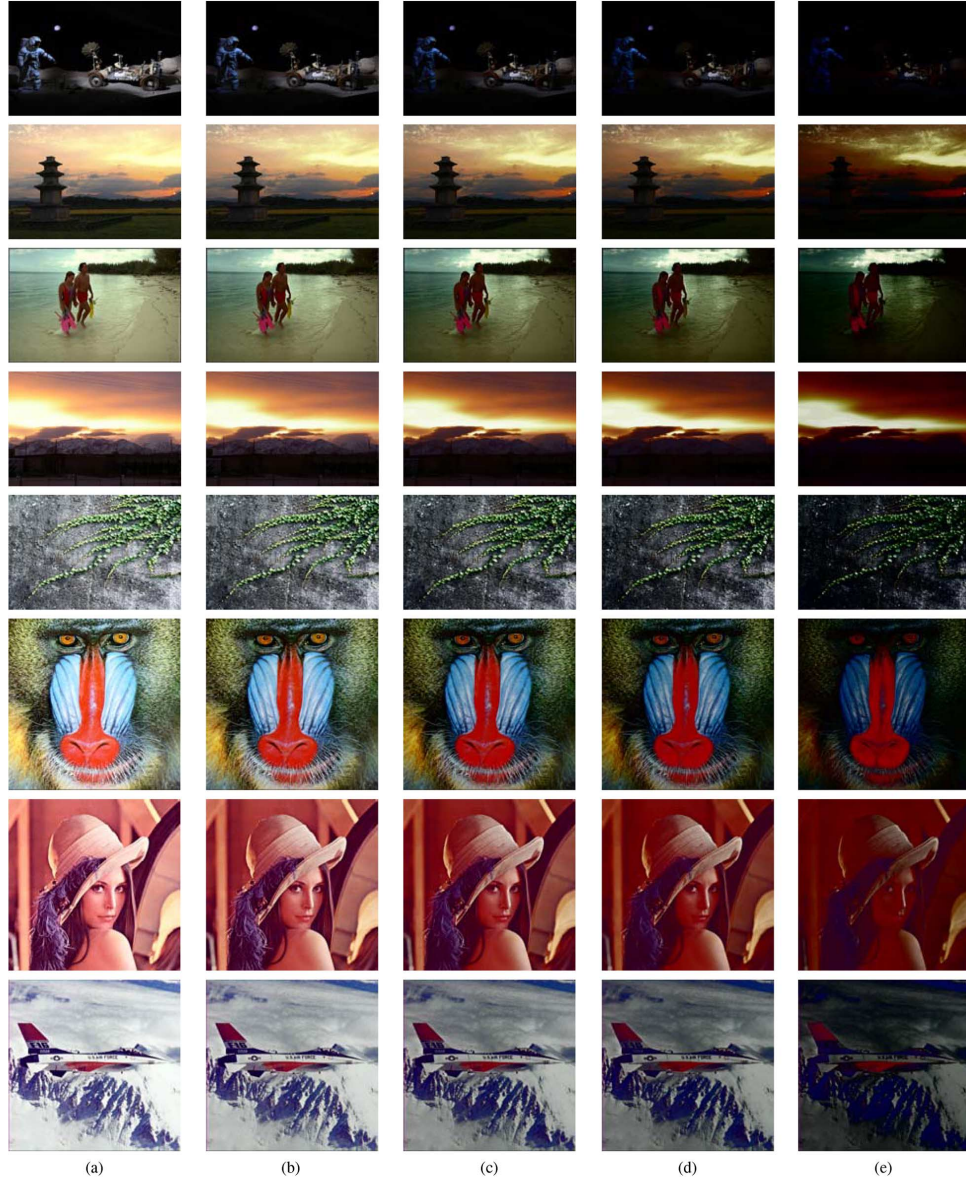


Fig. 6. PCCE results: (a) $\beta = 0$, (b) $\beta = 0.5$, (c) $\beta = 1.5$, (d) $\beta = 3$, and (e) $\beta = 15$.

visual details partly, but the other relatively dark images are severely degraded. In general, β can be set to a higher number for a brighter image to save power more aggressively. On the other hand, for a dark input image, β should be less than 2 for the proposed algorithm to yield good image quality.

Fig. 7 shows how the transformation functions vary according to β . As β gets larger, the proposed algorithm lowers the transformation functions to save more power, but it preserves the slopes of the functions (or, equivalently, the contrast) for input-pixel values with large histogram values. However, as β gets larger, the proposed algorithm inevitably reduces the contrast for infrequent input-pixel values. For example, “Pagoda” has low histogram values for input-pixel values around 90. Thus, at $\beta = 3$, the transformation function becomes flat near those pixel values.

Fig. 8 compares the TDP measurements for the images in Figs. 4 and 6. For the dark “Moon” image, all three contrast-enhancement methods HE, WAHE, and the proposed algorithm

($\beta = 0$) increase pixel values to stretch the image contrast, requiring higher TDPs than the original input images. However, the proposed algorithm can reduce TDPs by increasing parameter β . Moreover, for brighter images, such as “Beach” and “Ivy,” the proposed algorithm can reduce the power consumption more significantly while improving the overall contrast. For instance, on the “Ivy” image, the proposed algorithm at $\beta = 1.5$ reduces the TDP by more than 70%, as compared with the input image, but it still improves the contrast.

Fig. 9 compares the outputs of the proposed algorithm at $\beta = 1.5$ with those of the linear mapping method. Let us recall that the power-reduction ratio is defined as $\kappa = \text{TDP}_{\text{out}}/\text{TDP}_{\text{in}}$ in (32). The linear mapping method uses a linear transformation function $x_k = c \cdot k$, where constant c is set for each image in such a way that the method achieves the same κ as the proposed algorithm. Whereas the linear mapping method provides dull output images due to the reduced dynamic ranges, the proposed algorithm provides significantly better image contrast and percep-

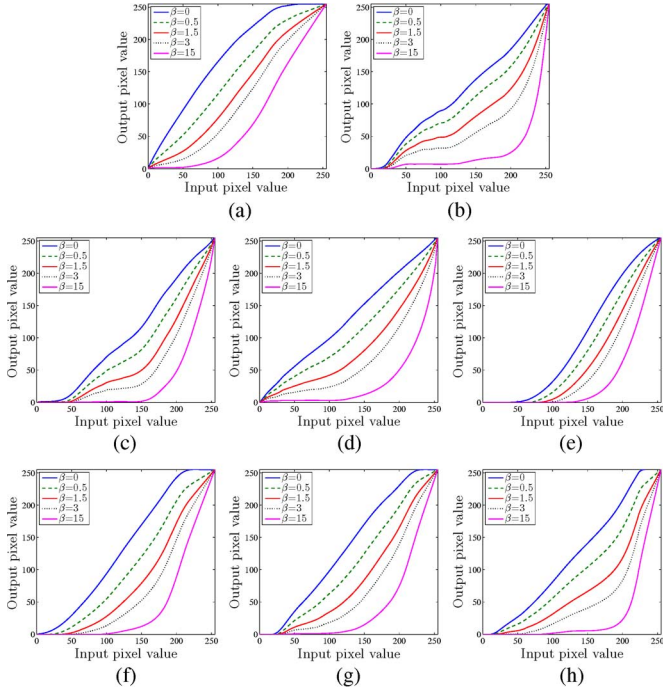


Fig. 7. Transformation functions for obtaining the PCCE results in Fig. 6. (a) Moon. (b) Pagoda. (c) Beach. (d) Sunset. (e) Ivy. (f) Baboon. (g) Lena. (h) F-16.

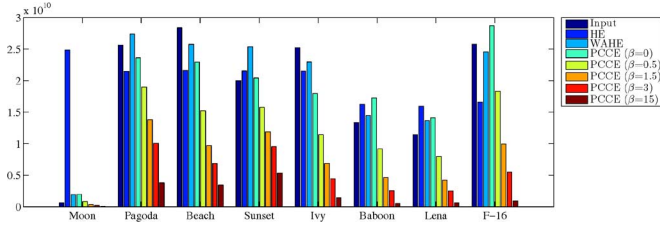


Fig. 8. TDP measurements of the images in Figs. 4 and 6.

tual quality. An exception is the “Sunset” image, on which the proposed algorithm sacrifices the details in the mountain region to improve the contrast in the sky region. In this test ($\beta = 1.5$), the mean and the variance of the power-reduction ratios κ for the eight test images are 0.36 and 0.009, respectively. At $\beta = 3$, the mean becomes 0.26, and the variance becomes 0.015. At $\beta = 15$, the mean is 0.14, and the variance is 0.010.

C. Impacts of Parameters β and μ on Power Consumption

As discussed in the last section, β is directly related to the power consumption. However, the LHM parameter μ also affects the power consumption since it influences the transformation function, as illustrated in Fig. 1. In Figs. 10 and 11, we show the output images and the power-reduction ratios κ for various combinations of β and μ . In both Figs. 10 and 11, it can be observed that, for fixed μ , TDP_{out} consistently decreases as β gets larger. On the contrary, the effects of μ on TDP_{out} are inconsistent, depending on the characteristics of the input images. Larger μ modifies the input histograms less strongly and overstretches the contrast. Because of the contrast overstretching, larger μ increases TDP_{out} on the dark “Eiffel Tower” image but decreases TDP_{out} on the bright “F-16” image. These inconsistent effects make μ less suitable for the power control.

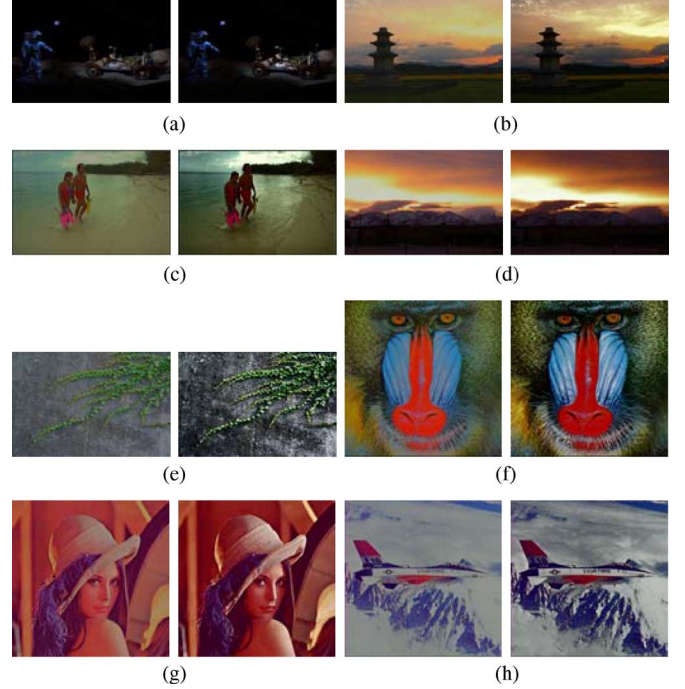


Fig. 9. Comparison of power-reduced output images obtained by the linear mapping method and the proposed algorithm ($\beta = 1.5$). In each subfigure, the left image is obtained by the linear mapping method, and the right one by the proposed algorithm. (a) Moon ($\kappa = 0.576$). (b) Pagoda ($\kappa = 0.540$). (c) Beach ($\kappa = 0.342$). (d) Sunset ($\kappa = 0.594$). (e) Ivy ($\kappa = 0.271$). (f) Baboon ($\kappa = 0.345$). (g) Lena ($\kappa = 0.369$). (h) F-16 ($\kappa = 0.385$).

The LHM parameter μ controls the level of contrast enhancement, but larger μ does not always provide better subjective quality. In the extreme case $\mu = \infty$, the histogram is not modified at all, and LHM becomes the conventional HE algorithm, which has several drawbacks. In Section V-A, we showed that, when μ is fixed to 5, the proposed algorithm without the power constraint suppresses the drawbacks of the conventional HE and provides good image quality reliably. Similarly, Figs. 10 and 11 show that case $\mu = 5$, enclosed by the solid rectangle, yields satisfactory image quality for various β values. In other words, each image within the rectangle provides comparable or better quality than the images outside the rectangle with similar power-reduction ratios. An improper value of μ may yield undesirable artifacts in the output image. Therefore, we suggest fixing μ to 5 and varying only β to control the power consumption.

D. PCCE for Video Sequences

Next, we enhance video sequences using the algorithm in Section IV. Two video clips from the movies “Avatar” and “The Shawshank Redemption” are employed as test sequences, and each clip consists of 700 frames. In the video enhancement, the power consumption is affected by the LHM parameter μ and the power-control parameter ρ in (33). However, as mentioned in the last section, μ is not suitable for the power control. Therefore, we fix μ to 5 and vary only ρ to control the power consumption.

Figs. 12 and 13 compare the TDPs of input and output frames. They also show selected frames. “Adaptive” denotes the proposed algorithm, and “Static” means the static method

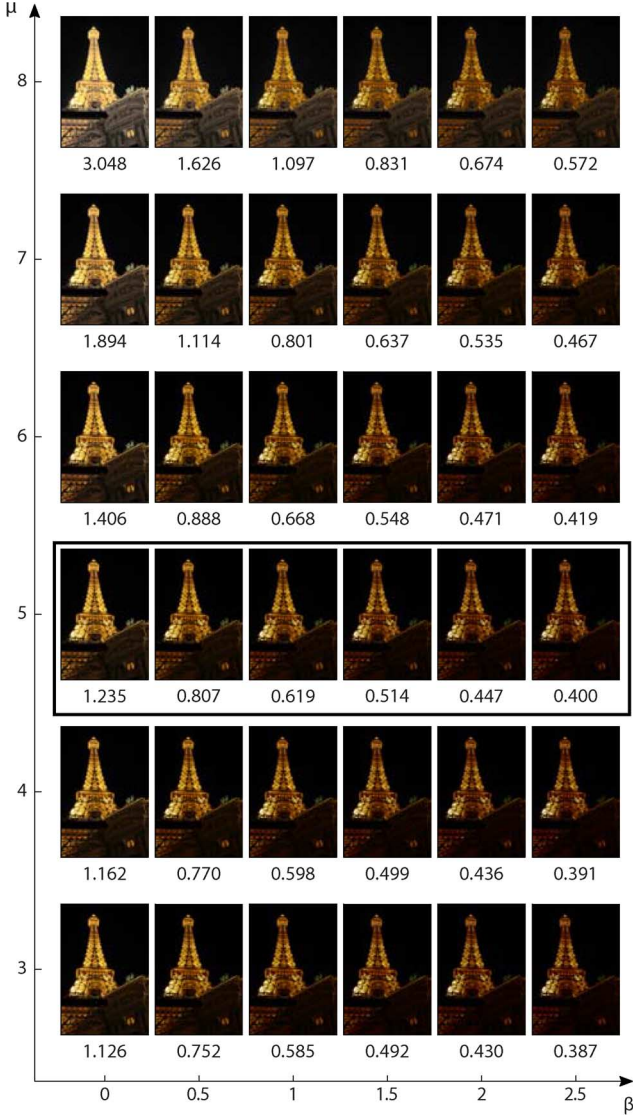


Fig. 10. Output “Eiffel Tower” images for various combinations of β and μ . Each number is the power-reduction ratio κ of the corresponding image. (Solid rectangle) To control the power consumption, we suggest fixing μ to 5 and varying only β .

that maintains a constant output TDP regardless of an input TDP. Let us first compare the proposed algorithm at $\rho = 0.5$ with the static method. The constant output TDP of the static method is set to be equal to the average TDP of the proposed algorithm at $\rho = 0.5$ over all frames. The proposed algorithm reduces more power for brighter input frames adaptively, whereas the static method fixes the output power and thus even increases power for some dark input frames. We see that the proposed algorithm provides better perceptual image quality. For bright input frames, e.g., the 200th frame in Fig. 12 and the 693rd frame in Fig. 13, the proposed algorithm reduces the power consumption by 26.8% and 11.8%, respectively, without decreasing the image quality. On the contrary, the static method darkens those frames too much and hides the details. For dark input frames, the proposed algorithm decreases the power consumption slightly, whereas the static method increases the power consumption. For instance, on the 135th

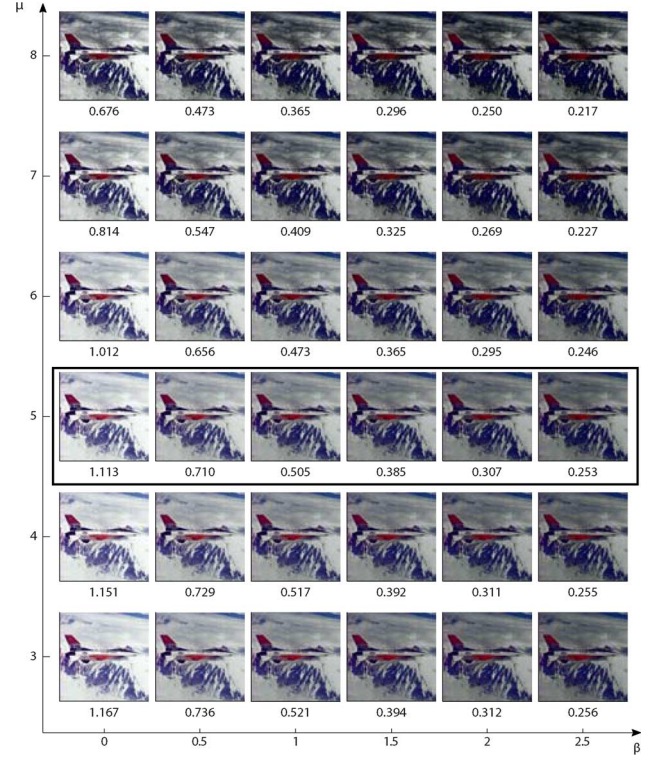


Fig. 11. Output “F-16” images and the power-reduction ratios for various combinations of β and μ . Each number is the power-reduction ratio κ of the corresponding image. (Solid rectangle) To control the power consumption, we suggest fixing μ to 5 and varying only β .

TABLE I
AVERAGE COMPUTATIONAL COMPLEXITY TO PROCESS A STILL IMAGE OR A VIDEO FRAME

	# of bisection iterations	# of variable changes	# of secant iterations	Processing time
Still image	-	16.9	3.84	6.23 ms
Video frame	9.34	5.37	2.65	15.12 ms

frame in Fig. 12, the static method consumes TDP about twice higher than the input frame but improves the image contrast only marginally.

In Figs. 12 and 13, we also see that the proposed algorithm saves more power, as parameter ρ gets larger. On average, when ρ is set to 0.5, 1.0, and 1.5, the proposed algorithm reduces the power consumption by 19.3%, 34.7%, and 46.9% for “Avatar” and by 21.2%, 36.3%, and 47.4% for “Shawshank Redemption,” respectively. The proposed algorithm saves more power for a brighter input frame, whereas it attempts to avoid the brightness reduction for a darker frame. Thus, although the proposed algorithm reduces the average power consumption significantly, it provides good subjective image quality by exploiting the characteristics of input frames.

E. Computational Complexity

Table I summarizes the computational complexity, which is required for the proposed PCCE algorithm to process a still image or a video frame. It lists the average performance over all

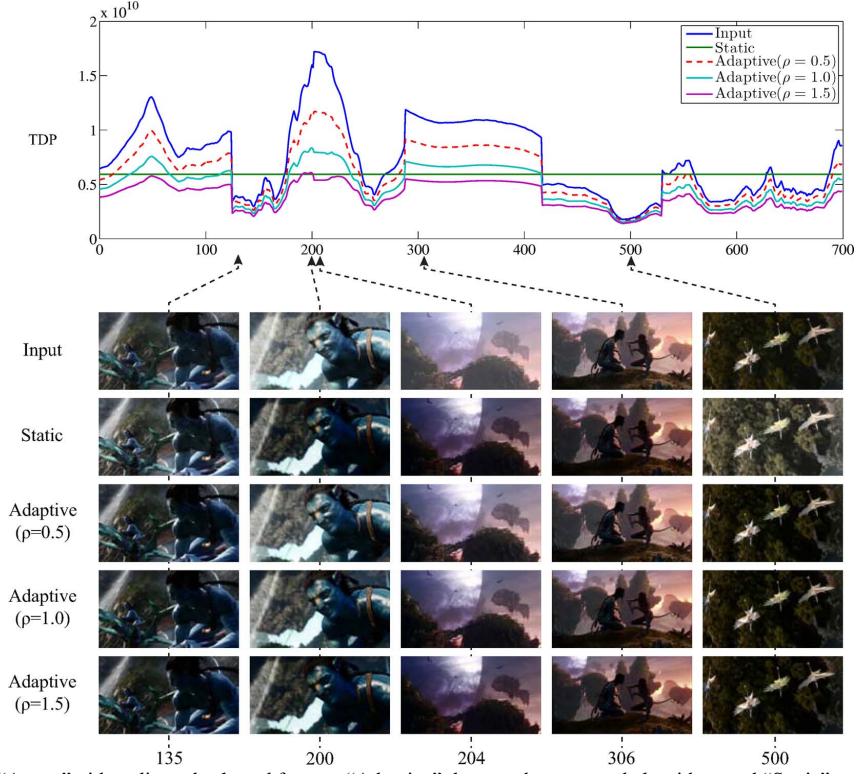


Fig. 12. TDP graphs for the “Avatar” video clip and selected frames. “Adaptive” denotes the proposed algorithm, and “Static” means the method that maintains a constant output TDP regardless of an input TDP. The constant TDP is set to be equal to the average TDP of the proposed algorithm at $\rho = 0.5$.

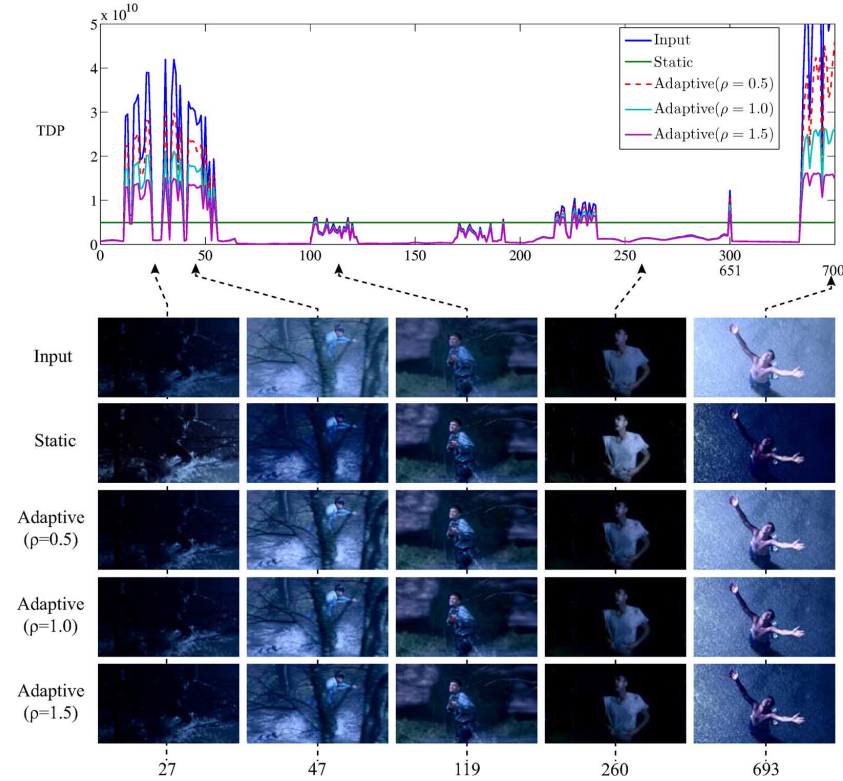


Fig. 13. TDP graphs for the “Shawshank Redemption” video clip and selected frames. In the graphs, the TDPs for frames 301 to 650 are omitted to show those for the other frames in greater detail. “Adaptive” denotes the proposed algorithm, and “Static” means the method that maintains a constant output TDP regardless of an input TDP. The constant TDP is set to be equal to the average TDP of the proposed algorithm at $\rho = 0.5$.

test images in Figs. 1, 4, and 10, as well as the average performance over all frames in the two video sequences in Figs. 12 and 13. We use a personal computer with a 3.3-GHz central processing unit for this test. The proposed algorithm is implemented in C but not optimized.

In the still image processing, the secant formula in (27) is iteratively applied to find a solution to $f(z) = 0$. The average number of secant iterations is about 3.84. As mentioned in the Appendix, if solution z is less than or equal to 0, we change z from y_{i-1} to y_i . The average number of variable changes is

16.9. The proposed algorithm takes only 6.23 ms to enhance a still image on the average.

In the video enhancement, for each frame, to find β that produces a target TDP_{out} , the proposed algorithm uses the bisection method, which requires additional iterations. Thus, the average processing time for a video frame is longer than that for a still image. However, both secant and bisection iterations are performed with vector \mathbf{y} , the dimension of which is just 256. Therefore, even our software implementation takes only 15.12 ms to process a video frame on the average. Moreover, the PCCE algorithm can be efficiently implemented on hardware such as field-programmable gate arrays.

VI. CONCLUSION

We have proposed the PCCE algorithm for emissive displays, which can enhance image contrast and reduce power consumption. We have made a power-consumption model and have formulated an objective function, which consists of the histogram-equalizing term and the power term. Specifically, we have stated the power-constrained image enhancement as a convex optimization problem and have derived an efficient algorithm to find the optimal transformation function. Simulation results have demonstrated that the proposed algorithm can reduce power consumption significantly while yielding satisfactory image quality. In this paper, we have employed the simple LHM scheme, which uses the same transformation function for all pixels in an image, for the purpose of the contrast enhancement. One of the future research issues is to generalize the power-constrained image enhancement framework to accommodate more sophisticated contrast-enhancement techniques, such as [10] and [11], which process an input image adaptively based on local characteristics.

APPENDIX

EXPRESSION OF ALL ELEMENTS IN \mathbf{y} IN TERMS OF A SINGLE VARIABLE z

Let us assume that $y_1 > 0$. The conditions in (21)–(23) can be rewritten as

$$y_i \geq 0, \quad \lambda_i \geq 0, \quad \text{and} \quad \lambda_i y_i = 0 \quad \text{for all } i. \quad (34)$$

Therefore, $\lambda_1 = 0$. Also, $y_2 = y_1 + \bar{m}_2 - \bar{m}_1 + (\alpha\gamma/2)h_1y_1^{\gamma-1} + (\lambda_2/2)$ from (25). Let us consider two cases.

$$\text{Case 1 : } y_1 + \bar{m}_2 - \bar{m}_1 + (\alpha\gamma/2)h_1y_1^{\gamma-1} > 0.$$

$$\text{Case 2 : } y_1 + \bar{m}_2 - \bar{m}_1 + (\alpha\gamma/2)h_1y_1^{\gamma-1} \leq 0.$$

In Case 1, $y_2 > (\lambda_2/2)$. Then, $(\lambda_2/2) = 0$ from the constraints in (34), and

$$y_2 = y_1 + \bar{m}_2 - \bar{m}_1 + \frac{\alpha\gamma}{2}h_1y_1^{\gamma-1}. \quad (35)$$

Also, from (25), $y_3 = y_2 + \bar{m}_3 - \bar{m}_2 + (\alpha\gamma/2)h_2(y_1 + y_2)^{\gamma-1} + (\lambda_3/2)$. We have two subcases.

$$\text{Case 1.1 : } y_2 + \bar{m}_3 - \bar{m}_2 + (\alpha\gamma/2)h_2(y_1 + y_2)^{\gamma-1} > 0.$$

$$\text{Case 1.2 : } y_2 + \bar{m}_3 - \bar{m}_2 + (\alpha\gamma/2)h_2(y_1 + y_2)^{\gamma-1} \leq 0.$$

In Case 1.1, $(\lambda_3/2) = 0$ and

$$y_3 = y_2 + \bar{m}_3 - \bar{m}_2 + \frac{\alpha\gamma}{2}h_2(y_1 + y_2)^{\gamma-1}. \quad (36)$$

By plugging (35) into (36), y_3 can be expressed in terms of y_1 . In Case 1.2, since $y_3 \leq (\lambda_3/2)$, $y_3^2 \leq (\lambda_3 y_3/2)$. Therefore, $y_3 = 0$.

In Case 2, $y_2 = y_1 + \bar{m}_2 - \bar{m}_1 + (\alpha\gamma/2)h_1y_1^{\gamma-1} + (\lambda_2/2) = 0$. From (25), $y_3 = \bar{m}_3 - \bar{m}_2 + (\alpha\gamma/2)h_2y_1^{\gamma-1} + (\lambda_3 - \lambda_2/2)$. By combining these two equations, we have $y_3 = y_1 + \bar{m}_3 - \bar{m}_1 + (\alpha\gamma/2)(h_1 + h_2)y_1^{\gamma-1} + (\lambda_3/2)$. We again have two subclasses

$$\text{Case 2.1 : } y_1 + \bar{m}_3 - \bar{m}_1 + (\alpha\gamma/2)(h_1 + h_2)y_1^{\gamma-1} > 0.$$

$$\text{Case 2.2 : } y_1 + \bar{m}_3 - \bar{m}_1 + (\alpha\gamma/2)(h_1 + h_2)y_1^{\gamma-1} \leq 0.$$

In Case 2.1, $(\lambda_3/2) = 0$ and

$$y_3 = y_1 + \bar{m}_3 - \bar{m}_1 + \frac{\alpha\gamma}{2}(h_1 + h_2)y_1^{\gamma-1}. \quad (37)$$

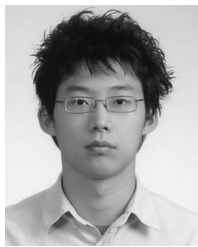
In Case 2.2, $y_3 = 0$.

Consequently, in all cases, y_2 and y_3 are either 0 or expressed in terms of a single variable y_1 . Similarly, all the other elements in \mathbf{y} can be also expressed in terms of a single variable $z = y_1$. Therefore, we can obtain function $f(z)$ in (26) and solve $f(z) = 0$ using the secant method. If solution $z = y_1$ is less than or equal to 0, it violates the starting assumption in this Appendix. In such a case, we set y_1 to 0, express all the other elements y_i by variable $z = y_2$, and solve $f(z) = 0$. We continue this procedure until we find the first positive $z = y_i$ that expresses the subsequent elements and solves equation $f(z) = 0$.

REFERENCES

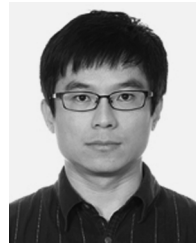
- [1] R. C. Gonzalez and R. E. Woods, *Digital Image Processing*, 3rd ed. Upper Saddle River, NJ: Prentice-Hall, 2007.
- [2] W.-C. Cheng, Y. Hou, and M. Pedram, "Power minimization in a backlit TFT-LCD display by concurrent brightness and contrast scaling," *IEEE Trans. Consum. Electron.*, vol. 50, no. 1, pp. 25–32, Feb. 2004.
- [3] P.-S. Tsai, C.-K. Liang, T.-H. Huang, and H. H. Chen, "Image enhancement for backlight-scaled TFT-LCD displays," *IEEE Trans. Circuits Syst. Video Technol.*, vol. 19, no. 4, pp. 574–583, Apr. 2009.
- [4] W. Den Boer, *Active Matrix Liquid Crystal Displays*. Amsterdam, The Netherlands: Newnes, 2005.
- [5] S. R. Forrest, "The road to high efficiency organic light emitting devices," *Org. Electron.*, vol. 4, no. 2/3, pp. 45–48, Sep. 2003.
- [6] B. Young, "OLEDs—Promises, myths, and TVs," *Inf. Display*, vol. 25, no. 9, pp. 14–17, Sep. 2009.
- [7] H. D. Kim, H.-J. Chung, B. H. Berkeley, and S. S. Kim, "Emerging technologies for the commercialization of AMOLED TVs," *Inf. Display*, vol. 25, no. 9, pp. 18–22, Sep. 2009.
- [8] I. Choi, H. Shim, and N. Chang, "Low-power color TFT LCD display for hand-held embedded systems," in *Proc. Int. Symp. Low Power Electron. Des.*, 2002, pp. 112–117.
- [9] A. Iranli, H. Fatemi, and M. Pedram, "HEBS: Histogram equalization for backlight scaling," in *Proc. Des. Autom. Test Eur.*, Mar. 2005, pp. 346–351.
- [10] J. Stark, "Adaptive image contrast enhancement using generalizations of histogram equalization," *IEEE Trans. Image Process.*, vol. 9, no. 5, pp. 889–896, May 2000.
- [11] J.-Y. Kim, L.-S. Kim, and S.-H. Hwang, "An advanced contrast enhancement using partially overlapped sub-block histogram equalization," *IEEE Trans. Circuits Syst. Video Technol.*, vol. 11, no. 4, pp. 475–484, Apr. 2001.
- [12] Z. Yu and C. Bajaj, "A fast and adaptive method for image contrast enhancement," in *Proc. IEEE ICIP*, Oct. 2004, vol. 2, pp. 1001–1004.
- [13] T. K. Kim, J. K. Paik, and B. S. Kang, "Contrast enhancement system using spatially adaptive histogram equalization with temporal filtering," *IEEE Trans. Consum. Electron.*, vol. 44, no. 1, pp. 82–87, Feb. 1998.
- [14] Y.-T. Kim, "Contrast enhancement using brightness preserving bi-histogram equalization," *IEEE Trans. Consum. Electron.*, vol. 43, no. 1, pp. 1–8, Feb. 1997.
- [15] Y. Wang, Q. Chen, and B. Zhang, "Image enhancement based on equal area dualistic sub-image histogram equalization method," *IEEE Trans. Consum. Electron.*, vol. 45, no. 1, pp. 68–75, Feb. 1999.

- [16] Q. Wang and R. K. Ward, "Fast image/video contrast enhancement based on weighted thresholded histogram equalization," *IEEE Trans. Consum. Electron.*, vol. 53, no. 2, pp. 757–764, May 2007.
- [17] T. Arici, S. Dikbas, and Y. Altunbasak, "A histogram modification framework and its application for image contrast enhancement," *IEEE Trans. Image Process.*, vol. 18, no. 9, pp. 1921–1935, Sep. 2009.
- [18] G. Sapiro and V. Caselles, "Histogram modification via partial differential equations," in *Proc. IEEE ICIP*, Oct. 1995, vol. 3, pp. 632–635.
- [19] V. Caselles, J.-L. Lisani, J.-M. Morel, and G. Sapiro, "Shape preserving local histogram modification," *IEEE Trans. Image Process.*, vol. 8, no. 2, pp. 220–230, Feb. 1999.
- [20] F. Drago, K. Myszkowski, T. Annen, and N. Chiba, "Adaptive logarithmic mapping for displaying high contrast scenes," *Comput. Graph. Forum*, vol. 22, no. 3, pp. 419–426, Sep. 2003.
- [21] S. Boyd and L. Vandenberghe, *Convex Optimization*. Cambridge, U.K.: Cambridge Univ. Press, 2004.
- [22] M. Dong, Y.-S. K. Choi, and L. Zhong, "Power modeling of graphical user interfaces on OLED displays," in *Proc. Des. Autom. Conf.*, Jul. 2009, pp. 652–657.
- [23] C. Poynton, *A Technical Introduction to Digital Video*. Hoboken, NJ: Wiley, 1996.
- [24] M. Rose, C. Main, Y. Fan, S. Percheyev, Z. Shaikh, and S. Silva, "Laser processed hydrogenated amorphous silicon for field emission displays," *J. Optoelectron. Adv. Mater.*, vol. 11, no. 9, pp. 1037–1043, Sep. 2009.
- [25] W. Press, S. Teukolsky, W. Vetterling, and B. Flannery, *Numerical Recipes in C: The Art of Scientific Computing*, 2nd ed. Cambridge, U.K.: Cambridge Univ. Press, 1992.
- [26] C. Lee, C. Lee, and C.-S. Kim, "Power-constrained contrast enhancement for OLED displays based on histogram equalization," in *Proc. IEEE ICIP*, Sep. 2010, pp. 1689–1692.
- [27] R. L. Burden and J. D. Faires, *Numerical Analysis*, 8th ed. Pacific Grove, CA: Brooks/Cole, 2005.



Chulwoo Lee received the B.S. degree in electrical engineering from Korea University, Seoul, Korea, in 2008, where he is currently working toward the Ph.D. degree in electrical engineering.

His research topics include power-constrained image/video enhancement and high dynamic range imaging.



Chul Lee (S'06) received the B.S. and M.S. degrees in electrical engineering from Korea University, Seoul, Korea, in 2003 and 2008, respectively, where he is currently working toward the Ph.D. degree in electrical engineering.

From 2002 to 2006, he was with Biospace Inc., Seoul, Korea, where he was involved in the development of medical equipment. His research interests are image restoration and high-dynamic-range imaging.



Young-Yoon Lee (M'11) received the B.S. (*summa cum laude*) and Ph.D. degrees in electrical engineering from Seoul National University, Seoul, Korea, in 1999 and 2008, respectively.

Since 2008, he has been working as a Senior Engineer with Digital Media and Communications Research and Development Center, Samsung Electronics Company, Ltd., Suwon, Korea. His research interests include image and video compression, and multimedia watermarking, medical imaging, information theory, and applied mathematics.

Dr. Lee was the recipient of a Korea Foundation for Advanced Studies Scholarship from 2000 to 2003.



Chang-Su Kim (S'95–M'01–SM'05) received the B.S. and M.S. degrees in control and instrumentation and the Ph.D. degree in electrical engineering with a Distinguished Dissertation Award from Seoul National University (SNU), Seoul, Korea, in 1994, 1996, and 2000, respectively.

From 2000 to 2001, he was a Visiting Scholar with the Signal and Image Processing Institute, University of Southern California, Los Angeles, and a Consultant for InterVideo Inc., Los Angeles. From 2001 to 2003, he coordinated the 3-D Data Compression

Group in the National Research Laboratory for 3-D Visual Information Processing, SNU. From 2003 and 2005, he was an Assistant Professor in the Department of Information Engineering, Chinese University of Hong Kong. Since 2005, he has been with the School of Electrical Engineering, Korea University, Seoul, Korea, where he is currently an Associate Professor. He has published more than 150 technical papers in international journals and conferences. His research topics include image, video, and 3-D graphics processing and multimedia communications.

Dr. Kim is an Editorial Board Member of the *Journal of Visual Communication and Image Representation*. In 2009, he received the Institute of Electronics Engineers of Korea/IEEE Joint Award for the Young Information Technology Engineer of the Year.